RSC Advances

# "Nose to brain delivery of astaxanthin loaded solid lipid nanoparticles: fabrication, radio labeling, optimization and biological studies"

| | |
|---|---|
| Journal: | *RSC Advances* |
| Manuscript ID | RA-ART-09-2015-019113.R1 |
| Article Type: | Paper |
| Date Submitted by the Author: | 15-Dec-2015 |
| Complete List of Authors: | Bhatt, Prakash; Jamia Hamdard, Pharmacognosy and phytochemistry<br>Srivastava, Pranay; Indian Institute of Toxicology Research, Developmental Toxicology Division<br>Pandey, Preeti; Kumaon University,<br>Khan, Washim; National Institute of Biologicals, The Biochemical Kit Laboratory<br>Panda, Bibhu; Jamia Hamdard, Pharmacognosy and phytochemistry |
| Subject area & keyword: | Nanomaterials - Materials < Materials |
| | |

SCHOLARONE™
Manuscripts

# Nose to brain delivery of astaxanthin loaded solid lipid nanoparticles: fabrication, radio labeling, optimization and biological studies

Prakash Chandra Bhatt[1], Pranay Srivastava[2], Preeti Pandey[3], Washim Khan[4], & Bibhu Prasad Panda [1†]

[1] Microbial and Pharmaceutical Biotechnology Laboratory, Centre for Advances Research in Pharmaceutical Sciences, Faculty of Pharmacy, Jamia Hamdard, Hamdard Nagar, New Delhi- 110062, India.

[2] Developmental Toxicology Division, Indian Institute of Toxicology Research Mahatma Gandhi Marg, Qaiserbagh, Lucknow, Uttar Pradesh- 226001, India.

[3] Department of Pharmaceutical Sciences, Bhimtal Campus, Kumaon University, Nainital- 263136, India

[4] Biochemical Kit Division, National Institute of Biology, Noida, Uttar Pradesh

[†]**Author for Correspondence:**

Dr. Bibhu Prasad Panda (M.Pharm., Ph.D.)
Assistant professor (Pharmaceutical Biotechnology)
Microbial and Pharmaceutical Biotechnology Laboratory,
Centre for Advances Research in Pharmaceutical Sciences,
Faculty of Pharmacy, Jamia Hamdard, Hamdard Nagar,
New Delhi- 110062, India
Email: bibhu_panda31@rediffmail.com
Mobile: +919990335013

## Abstract

The present study has been carried out to investigate intranasal delivery of astaxanthin as solid lipid nanoparticles with an intention to improve brain targeting of astaxanthin for neurological disorders. The astaxanthin solid lipid nanoparticles were prepared by double emulsion solvent displaces method. In addition to statistical analysis using response surface methodology showed that optimum values of stearic acid (50 mg), % of drug (6.11%) and a ratio of surfactant to co-surfactant (Poloxamer 188: Lecithin (1:6) resulted 213.23 nm particle size and 0.367 poly dispersity index of the astaxanthin solid lipid nanoparticles. Radio labeling studies were performed by using technetium 99 to evaluate the biodistribution pattern after administration through different routes in experimental subjects. Radiolabeled nanoparticles were found to be 96 to 98% stable even after 48 hours of labeling in phosphate-buffered saline (pH 7.4). Comparative biodistribution data indicated that the higher drug concentration in the brain was achieved by intranasal administration of 99mTechnitium labeled astaxanthin solid lipid nanoparticles as compared to intravenous route, which was also confirmed by the gamma scintigraphy. Furthermore, studies on Pheochromocytoma12 cell line demonstrated the antioxidant potential of astaxanthin solid lipid nanoparticles against $H_2O_2$ induced toxicity. Our findings strongly emphasize that nanoparticle based nasal drug delivery of astaxanthin could impart utmost neuroprotection from oxidative stress in neurological disorders under in-vitro conditions.


**Keywords:** Astaxanthin, Nanoformulation, Radiolabeling, Biodistribution, Nose to brain.

# 1. Introduction

Astaxanthin (3, 3′-dihydroxy-β- β′-carotene-4-4′-dione) is one of the strong carotenoid found in aquatic animals such as crabs, salmon and mainly produced by micro-alga *Haematococcus pluvialis* and yeast *Phaffia rhodozyma.*[1] Astaxanthin has been found to exhibit 100 times more free radical scavenging activity than Vitamin E and 10 times than beta carotene.[2] The health benefits of astaxanthin include anti-aging, anticancer [3,4,5] and cardio-protective effects,[6] eye health[7] and protective effects on central nervous system.[8] Further it could readily neutralize free radicals and other reactive species by protecting the tissue from oxidative stress.[9]

Free Astaxanthin is highly unstable and poorly water soluble carotenoid. It can easily degrade with light, high temperature, oxygen. These limitations of the astaxanthin make it more difficult to formulate into a suitable dosage form. Evidence from various studies had shown potent antioxidant activity of astaxanthin and its efficacy against various disorders clinically, but absence of suitable formulation for site specific drug delivery mark the importance of this study.

Solid lipid nanoparticles (SLN) offer unique properties such as small size, large surface area, high drug loading and the interaction of phases at the interfaces, and are attractive for their potential to improve the performance of pharmaceuticals. [10] Due to their unique size dependent properties, lipid nanoparticles offer the possibility to develop new therapeutics. The ability of SLN to incorporate drugs into nanocarriers offers a new prototype in drug delivery that could be used for drug targeting. Hence solid lipid nanoparticles hold great promise for reaching the goals of controlled and site specific drug delivery. In addition solid lipid nanoparticles emerged as a promising strategy for the efficient delivery of hydrophobic drugs because of their versatile features and unique advantages. [10]

A very little effort has been made to formulate carotenoid particularly astaxanthin into a novel delivery system. In order to increase the thermal stability of astaxanthin various approaches have been utilized. Continuing with this Tachaprutinun *et al.,* (2009)[11] encapsulated astaxanthin into polymeric nanospheres by a solvent displacement

technique using high pressure homogenization technique, while astaxanthin nanoemulsion and nanodispersion were developed by Anarjan *et al.,* (2010).[12]

Of all the organs, the brain is considered to be a soft target for oxidative insult due to the presence of high levels of unsaturated fatty acids, iron, and rich irrigation with blood vessels. [13] As oxidative stress has been considered to be one of the factors accounting for pathogenesis of many neurodegenerative disorders including Alzheimer's disease and Parkinson's disease. Astaxanthin has the capacity to cross the blood brain barrier in mammals [14] makes it a promising candidate for the treatment of various neurological disorders. Research evidences suggest the neuroprotective potential of natural astaxanthin in neurodegenerative diseases. However, the lack of a suitable delivery system to penetrate the blood–brain barrier has led the failure to exhibit the same in the *in-vivo* models.

The rationale for selection of an intranasal route for the delivery of 99mTc-AST-SLN complex depends on the composition of intranasal route which offers many advantages. Intranasal route is composed of highly vascularized epithelium layer of nasal mucosa [15] and porous endothelial membrane along with its large surface area for rapid drug absorption with faster onset of action. Further this route has a lower enzyme level as compared to GIT tract and liver [15] along with high blood flow per $cm^3$ facilitates direct drug transport to the brain and systemic circulation thereby avoiding first pass metabolism and enhance bioavailability. In addition brain targeting through intra nasal route bring the drug in direct contact with the olfactory/or trigeminal nerve pathways which is located in the nasal cavity as the neuro-epithelium is the only part of central nervous system that is directly exposed to the external environment. Thus, better targeting can be done by direct delivery of drugs from sub-mucosal space of the nose into the brain.

Researchers have reported the formulation and evaluation of solid lipid nanoparticle for brain targeting [16] and their findings substantiate the existence of a direct nose to brain route for nanoparticles administered to the nasal cavity.

The aim of the present study was to develop solid lipid nanoparticle consisting sufficient amount of astraxanthin (AST-SLN) for various neurodegenerative disorders. Response-

Surface methodology (RSM) was used to develop empirically significant models for optimized quality attributes of AST-SLN namely average particle size, poly dispersity index and astaxanthin concentration of AST-SLN. In order to resolve the effect of formulation ingredients in physiochemical properties of astaxanthin nanoparticle numerous tools were employed out of which Box-Behnken's design was found to be substantially constructive.

Here, we report the development of solid lipid nanoparticles of astaxanthin (AST-SLN) using citric acid, lecithin and polaxamer 188 by the solvent displacement method. The formulation was optimized by response surface methodology and evaluated for particle size, loading capacity, entrapment efficiency and particle morphology. The optimized formulation was further studied for its bio distribution in different organs and tissues.*In vitro* system consisting of PC12 cell lines was utilized to study the effect of AST-SLN in $H_2O_2$ induced oxidative stress in pre-, post and co- treatment protocols.

## 2. Materials and methods

### 2.1. Chemicals and equipments

Astaxanthin derived from algal source was obtained as a gift sample from Algaltech, Israel. All the chemicals used for formulation development were procured from Merck, India. The animal cell media and reagents used for *in vitro* study were brought from Hi-media, India. The pheochromocytoma (PC 12) cell line was obtained from National Centre for Cell Sciences, Pune, India. Particle size and polydispersity index of the formulation were determined using the Zeta sizer Nano ZS (Malvern Instruments Limited, Worcestershire, UK). Microscopic analysis was performed using a LEO 435 V scanning electron microscope (Leo electron microscopy Ltd., Cambridge, UK) and TEM CM-10 (Philips, Netherlands). Radioactivity was measured by gamma ray spectrometer (GRS23C, Electronics Corporation of India Limited, India).Gamma imaging studies were carried out by single-photon emission computerized tomography (SPECT, LC 75-005, Diacam; Siemens AG, Erlanger, Germany). Multiwellmicroplate reader (Synergy HT, Bio-Tek Instruments, Inc. Vermont, USA) was used for colorimetric assay.

### 2.2. Preparation and optimisation of AST-SLN formulation

Astaxanthin solid lipid nanoparticles were prepared by the solvent displacement method as described by Ribeiro *et al*. 2008[17] with modifications. In brief, astaxanthin (10 mg) was incorporated in the organic phase before the addition of stearic acid and lecithin. The drug was solubilized followed by the addition of the lipids. The lipid, stearic acid and lecithin were taken in ratios of 1:1, 1:4, 1:3,1:5, 1:6 ,1:8 and among them 1:3 and 1:6 were selected and were dissolved in 10 ml of dichloromethane (organic phase) by slight heating at 50 °C on a hot plate. The aqueous phase was prepared by dissolving polaxamer 188 (1%) in 50 ml of distilled water. The organic phase was then taken into a syringe and injected into the aqueous phase (50 ml) in a slow, drop wise manner with stirring. The solution was stirred at 3000 G for 2 hours. The AST-SLNs were harvested by centrifuging at 11,000 G for 40 minutes at 4°C. The supernatant discarded and the pellet removed, washed with distilled water and dried to obtain the solid lipid nanoparticles. The formulations obtained were further optimized with Box-Behnken design using response surface methodology (RSM).

Concentration of lipid and concentration of the drug and the ratio of surfactant and co-surfactant was optimized for the formulation using RSM, in order to obtain solid lipid nano particles of natural astaxanthin. A total 17-run, 3-factor, 3-level Box-Behnken design was employed to construct quadratic models for the optimization process. This design was suitable for investigating the quadratic response surface and for constructing a second-order polynomial model using Design- Expert Software (v.8.0 software of Stat-ease Inc. USA). The design consisted of replicated center points and a set of points lying at the midpoints of each edge of the multidimensional cube, which defined the region of interest used to evaluate the main effects, interaction effects, and quadratic effects of the formulation ingredients, and to optimize the formulation. Factors evaluated in this study were the amount of lipid (A), % amount of drug (B), ratio of S mix (surfactant: co-surfactant) (C) as the independent variables which were represented by −1, 0 and +1, analogous to the low, middle, and high values respectively as described in Table 1. The studied dependent responses were particle size (PS) and poly dispersity index (PDI).

### 2.3. **Evaluation of the solid lipid nanoparticles**

The PS and PDI of the formulations were determined by dynamic light scattering technique. The entrapment efficiency and loading capacity of the astaxanthin SLN was determined by the separation of the astaxanthin from the drug entrapped in the SLN by centrifugation at 11,000 rpm for 40 min at 4°C. The supernatant containing the free astaxanthin was quantified by high performance liquid chromatography. The astaxanthin percentage drug loading (DL) and the entrapment efficiency (EE) were calculated. The percentage yield of the SLN was determined by dividing the practical weight of solid nanoparticles after centrifugation and freeze drying cycle by theoretical weight of nanoparticles. Theoretical weight was obtained by the sum of the weights of the entire solid component used in preparation of nanoparticles[18]. Particle surface morphology was evaluated by scanning electron and by transmission electron microscopy.

The release of astaxanthin from the SLN's was studied using the Dialysis Method in pH 7.4 phosphate buffer. The aliquots so obtained at each time point were analyzed for drug released as a function of time. [19]

### 2.3.1 Particle size and PDI Determination of AST-SLN

The average of the particle size and polydispersity index (PDI) measured by using the Zetasizer (Nano-ZS, Malvern Instruments) and analyzed by "DTS nano" software. In brief, the prepared nanoparticles were harvested and washed by 5 successive cycles of centrifugation at 4°C and redispersion cycles in deionized water at 11000 rpm for 30 min. Several cycles of washing with deionized water was performed to ensure the complete removal of free drug and residual surfactants. The particles were dispersed in a low volume of water and lyophilized for 24 h to obtain powdered and stabilized nanoparticles. The final product was stored at -20°C until used for further characterization.

The particle size and the polydispersity index were measured by diluting the formulation with an aqueous phase (de-ionized water) up to 200 times followed by the vigorous shaking to obtain about 100-250 kilocounts per second.

### 2.3.2 Transmission Electron Microscope (TEM) of AST-SLN

Transmission Electron Microscope (TEM) was employed for the microscopic evaluation of optimized formulations using TEM CM-10 (Philips, Netherlands). In brief, for TEM evaluation a drop of formulation was applied on the carbon coated grid with 2% Phospho-tungestic acid (PTA) and it was left for 30 Sec. The dried, coated grid was taken to a slide and after placing the cover slip, observed under TEM operated at 60-80 KV.

### 2.3.3 Scanning Electron Microscopy (SEM) of AST-SLN

For SEM analysis of the freeze-dried nanoparticles, a random sample was mounted on an aluminum sample mount and sputter coated with gold- palladium alloy to minimize surface charging. SEM analysis was performed using a LEO 435 V scanning electron microscope (Leo electron microscopy Ltd., Cambridge, UK) at a working distance of 15 mm and an accelerating voltage of 15kV.

## 2.4 Radio labeling of AST-SLN

The AST-SLN was radiolabeled with Technetium-99m (99mTc) as per the method described by Theobald (1990). [20] The pertechnetate ($TcO^4$-) (2 mCi) was reduced with stannous chloride (in 10% acetic acid) and the pH was adjusted to 7.4 with 0.5 M sodium bicarbonate. To it was added the test formulation AST-SLN to be radiolabeled in a concentration of 1 mg/ml and incubated at room temperature for 10 min and checked for labeling efficiency.

## 2.5 Radio labeling Efficiency

The labeling efficiency of the 99mTc-labeled AST-NP was determined by instant thin layer chromatography (ITLC) using ITLC-SG mini strips as described by Banerjee et al. (2005).[21] Silica gel-coated fiber sheets were used for ascending thin layer chromatography. One to two microliters of labeled complex was put at the bottom of the strip and acetone was used as the mobile phase. The solvent front was allowed to reach up to a height of 8 cm from the origin and was then cut into two halves. Radioactivity was checked in each half by gamma ray spectrometer (GRS23C, Electronics Corporation of India Limited, India). Colloid formation was determined in solvent. The radiocolloids

remain at the bottom of the strip, while free pertechnetate and labeled complex migrate to the solvent front.

### 2.6 Radiochemical purity

The presence of radio colloids was determined by the previously reported method (Mishra *et al.* 1991)[22] by developing ITLC strip using pyridine: acetic acid: water in a ratio of 3:5:1:5. Reduced/hydrolyzed Tc-99m present in the preparation will remain at the point of application, while both the free Tc-99m pertechnetate and labeled complex migrates with solvent front. Thus ITLC strips were used to determine free Tc-99m and reduced/hydrolyzed technetium, and based on these two parameters labeling efficiency and purity was determined. Radio labeling efficiency and radiochemical purity were determined as follows.

### 2.7. *In vivo* and *in vitro* studies

#### 2.7.1 Bio-distribution study

The study was approved by the institutional animal ethics committee (IAEC), (173/CPCSEA) male albino Wistar rats, weighing 180–200 g were used. Animals were procured from the central animal house facility (Jamia Hamdard, New Delhi), weighed immediately on procurement and marked distinctly with picric acid solution for easy identification. Animals were divided in two groups (intravenous group and intranasal group) for four time points with each group containing 16 rats. Further, in each group, animals were divided into four subgroups of 4 animals for four different time points for dose administration via intravenous and intranasal routes. The radio-labeled and optimized SLNs with final radioactivity of 2 mCi/mL was prepared, The Intravenous group received 25 µl of astaxanthin (4mg/kg). The intranasal group received 10 µl of astaxanthin (4mg/kg) in each nostril. The dosing time was set at 0, 1, 2, 4, 24hr interval. The rats were anesthetized using chloroform at 1, 2, 4, and 24 h post-administration and blood sample was collected via cardiac puncture. Blood samples were transferred into pre weighed ria vials and reweighed. The samples were analyzed for radioactivity by the gamma-ray counter. Radioactivity in various samples was determined in the unit of counts. Along with the blood samples, the standard solution was also checked for its

radioactivity that accounted to standard counts. At the end of each time point (1, 2, 4, and 24 h), each rat was sacrificed humanly and various organs, including the heart, liver, lungs, kidneys, spleen, stomach, intestine and brain were then isolated. Each organ was weighed and radioactivity was determined using gamma-ray counter.

From this data, percent activity/gram organ (% A/G) was calculated,[22] by using Equation.

$$\% \text{ Radioactivity / gram of tissue} = \frac{\text{Counts in Sample}}{\text{Wt. of sample X total injected count}} \text{ X } 100$$

### 2.7.2. Gamma imaging studies

The Wistar albino rats (6 no.) weighing between 180-200 g were selected for the study. Radiolabeled drug formulation, 99mTc-AST-SLN (100mCi/50ml) containing Astaxanthin (equivalent to 1mg/kg body weight), was injected through the tail vein of Wistar albino rats. Similarly, radio labeled drug formulations, 99mTc-AST-SLN (100mCi/20ml) containing astaxanthin (equivalent to 1mg/kg body weight), was administered (10µl) in each nostril. Animals were sedated by giving intramuscular injections of 0.75 ml/Kg body weight of diazepam and 1 mg/Kg body weight of ketamine throughout the experiment and placed on the imaging board. Imaging was performed using single-photon emission computerized tomography (SPECT, LC 75- 005, Diacam; Siemens AG, Erlanger, Germany) gamma camera.[23] The scintigraphy images following intravenous administration of AST-SLN and intranasal administration were recorded using a dual head Hawkeye gamma camera system (GEMS, UK). All images were analyzed with inbuilt software Entegra Version-2.

### 2.7.3 *In vitro* evaluation of AST-SLN on PC12 cell lines against $H_2O_2$ induced oxidative damage

Rat pheochromocytoma cell line (PC12) cells, used in the present study were procured from National Centre for Cell Sciences, Pune, India**.** Cells were grown as per the standard protocol described by Greene *et al.* [24] Non cytotoxic dose of AST-SLN Formulations (5 and 10 µg/ml) were selected for the study. Responsiveness of PC12 cells to formulation

was detected by dividing them into three treatment schedules (a) cells treated with formulation for 24 hours prior to $H_2O_2$ insult for 12 hrs (post treatment group); (b) cells treated with formulation for 24 hours along with $H_2O_2$ insult for 12 hours (co exposure group/co treatment group); (c) cells treated with formulation for 24 hours following 12 hours of $H_2O_2$ insult (pretreatment group). Influence of formulation was evaluated by comparing the values of treatment groups with respective non-treated cells exposed to $H_2O_2$ only. Percentage cell viability was assessed using tetrazolium bromide salt (MTT assay).[25]

### 2.7.4 Estimation of Glutathione (GSH) levels

Glutathione (GSH) levels were assessed following the exposure to three treatment schedules as described above using commercially available kit (Glutathione Detection Kit, Catalog no. APT250, Chemicon, USA). Briefly, cells were exposed to hydrogen peroxide and astraxanthin formulation in three treatment schedules followed by centrifugation at 700 g for 2 min at $4^0$C and lysed by lysis buffer and centrifugation over again at 12,000 g for 10 min at $4^0$C and the supernatant was collected to give final samples. Lysed samples (90 ml/well) were relocated to 96 well black bottom plates and mixed with freshly prepared assay cocktail (10 ml) followed by incubation for 2 h. The plates were read at excitation wavelength 380 nm and emission wavelength 460 nm using a multiwell microplate reader for estimation of GSH levels. Results were expressed as percentage of controls.

### 2.7.5 Estimation of lipid peroxidation (LPO) levels

The extent of lipid peroxidation was estimated by commercially available kit (Cayman's Chemicals Kit catalog no. 705003, USA) according to the manufacturer's protocol. The cells exposed to hydrogen peroxide and astraxanthin formulation in three treatment schedules were harvested in chilled PBS by scraping and washed twice with PBS at $4^0$C for 6 min at 1,500 rpm. The cell pellet was then sonicated at 15 W for 10 s (3 cycles) to obtain the cell lysate, which were detected spectrophotometrically at 500 nm using thiocyanate ion as the chromogen. 13-HpODE (13-hydroperoxy-octadecadienoic acid) was used as a standard and results were expressed as percentage of control.

# 3. Results

## 3.1. Characterization and optimization of astaxanthin solid lipid nanoparticles

Optimization of nano formulation was carried out on the basis of particle size (PS) and poly dispersity index (PDI). Actual and predicted results for PS and PDI are presented in Table 2. The model generated, analyzed by design expert software and the actual and predicted results for particle size obtained resulted in a quadratic equation

$$\text{PS unit} = 682 + 742.675A + 123.825B - 48.225C + 72.775AB + 17.425AC - 246.475\,BC + 295.8375A^2 + 15.3875B^2 - 32.4125C^2$$

$$PDI = 0.224 - 0.00012A + 0.02725B + 0.044875C - 0.10825AB + 0.0635AC + 0.12275BC + 0.29475\,A^2 + 0.1985B^2 - 0.06375C^2$$

Three-dimensional (3D) response surface (A, C and E) and contour plots (B, D and F), showing the effects of lipid concentration (*A*), drug percentage (*B*) and surfactant ratio (*C*) and the effect of their reciprocal interaction of the dependent variables of the astaxanthin nano formulation has been represented in figure 1 (for PDI) and supplementary figure 1 (for PS).

The analysis of variance of the model for PS and PDI is represented in Table 3. Point prediction of the design expert software was used to determine the optimum value formulation factors for PDI and smaller particle size of the AST-SLN. Finally, the optimum values of Stearic acid (50 mg), % amount of drug (6.11%) and the ratio of S mix (Poloxamer 188: Lecithin (1:6) was obtained. These values predict 213.23 nm size and 0.367 PDI of the AST-SLN.

## 3.2. Validation of optimized model

The particles were found spherical in shape with uniform size distribution (Figure 2a, 2b). The optimized values of parameters were validated by formulation and an average 205.85 nm of particle size was obtained, indicating a 95.24 % validity of the predicted model. . The PDI was found to be 0.349 (Table 2). This shows that all the AST-SLNs had narrow size distribution. The developed AST-SLNs shows a mean percentage yield of

68.74 ± 1.74 %, entrapment efficiency of 77.42 ± 1.15 % and mean loading capacity of 47.63 ± 1.07 %. The scanning electron microscopy (SEM) and transmission electron microscopy (TEM) of prepared AST-SLNs shows that the particles were spherical in shape with the nano range (Figure 2b and 2c).

The presence of astaxanthin, produced a significant effect on the optimal formulation, but the design space was found to be robust enough to accommodate the drug. An entrapment efficiency of 77.42%, along with mean percentage yield of 68.74 ± 1.74, % and mean loading capacity of 47.63 ± 1.07 % was found for optimal formulation.

### 3.3. *In vitro* release of AST-SLN

The *In vitro* drug release data shows that the total amount of drug released at the end of 48 hrs was 81.40 % and the release pattern of the drug from the formulation was found to be sustained and controlled release (Fig 3). *In vitro* release of astaxanthin from all the tested formulations are represented supplementary figure 2.

### 3.4. Radiolabelling of optimized formulation

AST-SLNs were radio labeled with Technetium-99m (99mTc). The labeling efficiency of the 99mTc-labeled AST-SLNs was determined by instant thin layer chromatography (ITLC) using ITLC-SG mini strips and was found to be 96.82 % and the presence of radio colloids was found to be > 4 %. The radio labeled SLNs were 96 to 98% stable even after 48 hours of labeling in phosphate-buffered saline (pH 7.4).

### 3.5. Biodistribution studies

For the biodistribution study of AST-SLNs, it was administered through intravenous and intranasal route. At different time interval various organs, including the brain, intestine, stomach, kidneys, spleen, liver, lungs, heart, blood was examined and percent activity per gram of organ (% $Ag^{-1}$) was calculated and shown in Table 4 & 5. It can be clearly seen that the brain levels were higher while blood levels were less after intranasal administration as compared with intravenous route. Also, very large portion of the radioactivity was found in the lungs, liver, spleen, and kidneys through the intravenous route indicating rapid biodistribution, elimination, and the 99mTc-AST-SLN uptake.

However, very high radioactivity levels could be detected in the stomach with the biodistribution data that SLNs were effective in increasing the 99mTc-AST-SLN concentration in the brain. Bio-distribution studies in albino rats showed that 1 h post-administration, brain accumulation of AST-SLNs (i.n.) was found to be 1.70 ± 0.13 (more than 200%) as compared to 0.844 ± 0.12 for AST-SLN (i.v.) respectively. Thus Comparative biodistribution data indicate higher drug concentration in the brain was achieved by intranasal 99mTc-AST-SLN as compared with 99mTc-AST-SLN (i.v.) and gamma scientigraphy results were concordant with biodistribution data.

### 3.6. Gamma scientigraphy imaging

In order to visualize brain uptake following intranasal and intravenous administration of the 99mTc-AST-SLN formulation, gamma scintigraphy was performed 1 h after intranasal and intravenous administration of the 99mTc-AST-SLN for localization of the 99mTc-AST-SLN in different organ and tissues of experimental subject, as determined by gamma camera imaging, is shown in Figure 6. Gamma scientigraphy imaging of rats following intravenous and intranasal administration confirmed the localization of the drug in the brain. Thus, the biodistribution pattern seen on non-invasive imaging with 99mTc-AST-SLN was similar to the radiometric data obtained after sacrificing the animals (Figure 4).

### 3.7. *In-vitro* evaluation on rat pheochromocytoma (PC12) cell lines

In order to carry out *in vitro* experimentation dose standardization was carried out through MTT assay and on the basis of the result obtained (Figure 5) two doses were selected sequentially viz 5µg/ml and 10µg/ml. Treatment with $H_2O_2$ led to a significant decrease in viable cells in all three paradigms assessed through MTT assay, while significant protection was observed in cells pretreated with 5µg/ml and 10µg/ml of AST-SLN .

There was an increase of 65% percent viability of PC12 cells of negative control (untreated with AST-SLN) than the positive control (cells treated with $H_2O_2$ only). Among all tested concentration of AST-SLNs, 5µgml$^{-1}$ and 10 µgml$^{-1}$ showed 94.45 % and 96.21 % cell viability while 25 µgml$^{-1}$, 50 µgml$^{-1}$ , 100 µgml$^{-1}$ and 200 showed a

reduced cell viability less than 65% by MTT assay. Therefore AST-SLNs concentrations of 5µgml$^{-1}$ and 10 µgml$^{-1}$were selected for *in-vitro* test.

In pretreatment module PC12 cells were treated with AST-SLN formulation for 24 hours following 12 hours of $H_2O_2$ insult resulted in 86.89 % cell viability with 5 µgml$^{-1}$ dose of astaxanthin nanoformulation and 96.04 % cell viability with 10 µgml$^{-1}$ as compared with the only $H_2O_2$ treated group which resulted in 34.83 % cell viability (Figure 6).

In post treatment module PC12 cells were treated with formulation for 24 hours prior to $H_2O_2$ insult for 12 hours resulted in 42.44 % cell viability with 5 µgml$^{-1}$ dose of astaxanthin nanoformulation and 55.02 % cell viability with 10 µgml$^{-1}$ (Figure 6).

In co exposure module PC12 cells treated with formulation for 24 hours along with $H_2O_2$ insult for 12 hours resulted in 88.04 % cell viability with 5 µgml$^{-1}$ dose of astaxanthin nanoformulation and 94.57 % cell viability with 10 µgml$^{-1}$ (Figure 6).

### 3.8. Effect on glutathione levels

Effect of astraxanthin formulation on hydrogen peroxide induced alterations in the levels of intracellular GSH concentrations is summarized in Figure 7. Statistically significant decrease ($p<0.01$) in levels of GSH has been observed in comparison to control. Pretreatment with AST-SLN protected intracellular levels of GSH in both 5 µgml$^{-1}$ and 10 µgml$^{-1}$ ($p<0.01$). A similar trend of protection has been observed in post treatment module wherein AST-SLN showed therapeutic response upon hydrogen peroxide exposure but less in comparison to the pre treatment module. Significant increase ($p<0.05$) in levels of GHH has been found in groups co exposed with AST-SLN and $H_2O_2$ with both doses of AST-SLN.

### 3.9. Effect on lipid peroxidation

AST-SLN formulation showed its antioxidant properties by controlling the damage caused by $H_2O_2$ in all three paradigms in the study. A significant increase ($p<0.01$) in lipid peroxidation has been observed in the group exposed to $H_20_2$ in comparison to control. Exposure to AST-SLN resulted to decrease the enhanced lipid peroxidation levels in pretreatment (5 µgml$^{-1}$ ($p<0.05$); 10 µgml$^{-1}$ ($p<0.05$)), post treatment (5 µgml$^{-1}$

($p<0.05$); 10 $\mu gml^{-1}$ ($p<0.05$) and co treatment (5 $\mu gml^{-1}$ ($p<0.05$); 10 $\mu gml^{-1}$ ($p<0.05$) groups (Figure 8).

## 4. Discussion

Regarding the effect of independent variables such as lipid level, drug % and surfactant ratio on the overall responses such as PDI and PS, this study clearly showed that the physiochemical properties of nanoparticles were significantly influenced by these formulation ingredients (Table 2, Figure 1, and Supplementary Figure 1). In most cases, fitting of the second-order quadratic regression models with the experimental data were found to be highly adequate to describe the relationship between the formulation ingredients and the nanoparticles properties satisfactorily ($R^2> 0.98$). The quadratic effects of lipid concentration, drug % and the ratio of surfactant to co-surfactant, had significant ($p< 0.0001$) effects on all response variables studied.

A uniform distribution of radioactivity was observed throughout the body, including the brain, when 99mTc-AST-SLN was administered intravenously, indicating that SLNs could cross the BBB.[26] Moreover, intranasal administration further improved the brain uptake of the drug as compared with intravenous route due to direct nose-to-brain delivery, indicating that SLNs through intranasal route have been found to be effective for brain targeting. Thus, the combined results of bio-distribution and gamma scintigraphic imaging studies on 99mTc-AST-SLN conclusively prove that intranasal administration of SLNs is effective for brain-targeted delivery and has tremendous potential for delivery of drugs to the central nervous system.

Lipophilic drugs tend to show slow clearance because of their longer retention and wider distribution in the body, while, hydrophilic drugs show rapid clearance from the body.[27] Our data indicate that 99mTc-AST-SLN complex showed strong lipophilic characteristics. It rapidly reached the target area and was cleared in a sustained manner. A significant uptake of the 99mTc-AST-SLN antioxidant complex in various major organs can offer high value antioxidant therapy in cancer treatment through its unique antioxidant mechanism. Increased accumulation of the 99mTc-AST-SLN complex in stomach and intestine, because of its lipophilic nature, suggests that the most probable route of excretion of the 99mTc-AST-SLN complex and its metabolites was through the biliary and intestinal excretion.[27] However,

accumulation of this complex was also observed in the kidneys of the animals, which suggest that the drug complex also get excreted from the renal route. Thus, our study conclusively reports that AST-SLN has a wide spectrum of biodistribution throughout the body which can be attributed to the lipophillic nature of the drug as well as the ability of the astaxanthin solid lipid nanoparticles to cross the blood brain barrier and protect the brain from oxidative stress, could potentially provide valuable support for brain health.

Antioxidant potency of natural astaxanthin has been shown to be even better than that of β-carotene, zeaxanthin, canthaxanthin, vitamin C and vitamin E.[28] Astaxanthin has a singlet oxygen quenching activity over 500 times greater than that of α-tocopherol,[29] as well as a 100-fold greater activity than vitamin E in inhibiting lipid peroxidation.[30] In recent years, increasing studies on astaxanthin have also revealed such other pharmacological activities in inflammation, cancer and diabetes.[28] Astaxanthin has a protective effect in neuronal SHSY5Y cells exposed to oxidative damage.[31]

With this background the AST-SLN has been evaluated in *in vitro* paradigm against $H_2O_2$ induced cellular damage in order to justify the utilization of the formulation as therapeutic, prophylactic or as protective medication. Our findings are in accordance with the earlier in-vitro studies which suggest that Astaxanthin significantly inhibited apoptosis, mitochondrial abnormalities and intracellular ROS generation in neuronal SHSY5Y cells exposed to oxidative damage.[31, 32]

The neuroprotective effect of AST-SLN could be conferred upon its antioxidant potential and mitochondrial protection[31] therefore, it is suggested that AST-SLN may be an effective treatment for oxidative stress-associated neuro degeneration.

It is evident that tyrosine hydroxylase enzyme has been involved in biosynthesis of catecholamines which is a rate limiting step in the process.[33] Alteration in the level of the enzyme activity might lead to schizophrenia, Parkinson's disease etc.[34] $H_2O_2$ has been shown to modulate the level of tyrosine hydroxylase in PC-12 cells.[35] Various mechanisms have been proposed to demonstrate the mechanism of oxygen radical formation and involvement of tyrosine hydroxylase enzyme.[36] In context with our present study which focuses on anti-oxidant system and free radical scavenging, proves to be a perfect model to

verify the potency of AST-SLN. The result of the present study demonstrates that AST-SLN significantly protects PC-12 cells as well as altering the expression of TH enzyme evaluated in *in vitro* system. These results demonstrate an effective role of AST-SLN on *in vitro* neuroprotective efficacy against $H_2O_2$ induced cellular injury and its action on the modulation of tyrosine hydroxylase.

## 5. Conclusion

The AST-SLN has shown a strong neuroprotective effect against oxidative stress in neuronal cell lines. On the other hand, in-vivo model has shown a wide biodistribution pattern of AST-SLN in different organ and tissues which can be further studied for different type of cancer in these organs and tissues. The direct nose to brain delivery of the 99mTc-AST-SLN has been evident by gamma scientigraphy imaging and radiometric data after sacrificing the animal. These findings substantiate that nanoformulation can be effectively utilized for brain targeting and can offer a protection from various neurological disease conditions. Further AST-SLN can be studied in a neurodegenerative disease animal model to validate the in-vitro results which strongly suggest that astaxanthin can offer neuroprotection from oxidative stress induced cellular damage.

**Declaration of conflict of interest**

*The authors report no conflicts of interest.*

**Acknowledgment**

*All the authors express their sincere thanks to the University Grant Commission, Government of India for funding the research project under MRP scheme. The authors also like to thank Dr. A. K. Mishra Scientist 'G', Institute of Nuclear Medicine and Allied Sciences, Defense Research & Development Organization, Ministry of Defense, Government of India, for providing the laboratory facility to carry out the radio labeling studies and Alga Technologies Ltd., Israel for providing the astaxanthin as a gift sample.*

**References**

1. R. T. Lorenz and G. R. Cysewski, *Trends Biotechnol.*, 2000, **18**, 160-167.
2. W. Miki, *Pure Appl. Chem.,* 1991, **63**, 141-146.

3. P. N. Prabhu, P. Ashokkumar and G. Sudhandiran, *Fund. Clin. Pharmacol.*, 2009, **23**, 225-234.
4. D. N. Tripathi and G. B. Jena, *Mutat. Res*., 2010, **696**, 69-80.
5. P. Palozza, C. Torelli, A. Boninsegna, R. Simone, A. Catalano, M. C. Mele and N. Picci, *Cancer Lett.*, 2009, **283**, 108-117.
6. G. J. Gross and S. F. Lockwood, *Mol. Cell Biochem.,* 2005, **272**, 221-227.
7. K .E. Goodwill, C. Sabatier, C Marks, *Nat. Struct. Biol*., 1997, **4**, 585.
8. A. Satoh, S. Tsuji, Y. Okada, N. Murakami, M. Urami, K. Nakagawa, M. Ishikura, M. Katagiri, Y. Koga and T. Shirasawa, *J. Clin. Biochem. Nutr.*, 2009, **44**, 280-284.
9. M. Wolf, S. Asoh, H. Hiranuma, I. Ohsawa, K. Iio, A. Satou, M. Ishikura and S. Ohta, *J. Nutr. Biochem.*, 2010, **21**, 381-389.
10. A. Date and V. B. Patravale, *Curr. Opin. Colloid In.,* 2004, **9**, 222-235.
11. Tachaprutinun, T. Udomsup, C. Luadthong and S. Wanichwecharungruang, *Int. J. Pharm.*, 2009, **374**, 119-124.
12. N. Anarjan, H. Mirhosseini, B. S. Baharin and C. P. Tan, *Food Chem.*, 2010, **123**, 477-483.
13. F. Facchinetti, V. L. Dawson and T. M. Dawson, *Cell Mol. Neurobiol.*, 1998, **18**, 667-682.
14. M.O.M. Tso and T.T. Lam, US5527533. (1996).
15. V. Pardeshi and V. S. Belgamwar, *Expert Opin. Drug Deliv.,* 2013, **10**, 957-972.
16. S. Patel, S. Chavhan, H. Soni, A. K. Babbar, R. Mathur, A. K. Mishra and K. Sawant, *J. Drug Target*, 2011, **19**, 468-474.
17. H. S. Ribeiro, B.-S. Chu, S. Ichikawa and M. Nakajima, *Food Hydrocolloid.,* 2008, **22**, 12-17.
18. Y. Baimark and Y. Srisuwan, *Nanoscale Res. Lett*., 2012,**7**, 271.
19. H. Zhang, F. M. Zhang and S. J. Yan, *Int. J. Nanomedicine*, 2012, **7**, 2901-2910.
20. Theobald AE. Textbook of Radiopharmacy: Theory and Practice In: Sampson CB (Ed.), New York, Gordon and Breach, 1990, 27-129.
21. T. Banerjee, A. K. Singh, R. K. Sharma and A. N. Maitra, *Int. J. Pharm.*, 2005, **289**, 189-195.

22. P. Mishra, A. Babbar and U. P. Chauhan, *Nucl. Med. Commun.*, 1991, **12**, 467-469.
23. J. M. Koziara, P. R. Lockman, D. D. Allen and R. J. Mumper, *Pharm. Res.*, 2003, **20**, 1772-1778.
24. L. A. Greene and A. S. Tischler, *P. Natl. Acad. Sci. USA.,*1976, **73**, 2424-2428.
25. M. A. Siddiqui, G. Singh, M. P. Kashyap, V. K. Khanna, S. Yadav, D. Chandra and A. B. Pant, *Toxicol. In Vitro,* 2008, **22**, 1681-1688.
26. S. C. Yang, L. F. Lu, Y. Cai, J. B. Zhu, B. W. Liang and C. Z. Yang, *J. Control Release*, 1999, **59**, 299-307.
27. O.J. Torrissen, K. Ingebrigtsen, *Aquaculture*, 1992, **108**, 381-385.
28. F. J. Pashkow, D. G. Watumull and C. L. Campbell, *Am. J. Cardiol.*, 2008, **101**, 58d-68d.
29. N. Shimidzu, M. Goto and W. Miki, *Fisheries Sci.*, 1996, **62**, 134-137.
30. M. Kurashige, E. Okimasu, M. Inoue and K. Utsumi, *Physiol. Chem. Phys. Med. NMR.,* 1990, **22**, 27-38.
31. X. Liu, T. Shibata, S. Hisaka and T. Osawa, *Brain Res.*, 2009, **1254**, 18-27.
32. X. B. Liu and T. Osawa, *Forum Nutr.*, 2009, **61**, 129-135.
33. T. Nagatsu, M. Levitt and S. Udenfriend, *J. Biol. Chem.*, 1964, **239**, 2910-2917.
34. K. E. Goodwill, C. Sabatier, C. Marks, R. Raag, P. F. Fitzpatrick and R. C. Stevens, *Nat. Struct. Biol.,* 1997, **4**, 578-585.
35. S. L. Kroll and M. F. Czyzyk-Krzeska, *Am. J. Physiol.*, 1998, **274**, C167-174.
36. J. D. Adams, Jr., L. K. Klaidman and P. Ribeiro, *Redox Rep.*, 1997, **3**, 273-279.

## Tables Legend

**Table 1:** Levels of formulation parameters (A) lipid concentration (B) Amount of drug % (C) surfactant ratio used in Box-Behnken's response surface design of astaxanthin solid lipid nanoparticles

**Table 2:** Box-Behnken's design with actual and predicted values of particle size and polydispersity index for astaxanthin solid lipid nanoparticles

**Table 3:** Analysis of variance of calculated model of astaxanthin solid lipid nanoparticles for particle size and poly dispersity index (PDI)

**Table 4:** Bio-distribution of 99mTc AST-SLN in Wister rats following intranasal administration for 1-24 hours at different time intervals

**Table 5:** Bio-distribution of 99mTc AST-SLN in Wister rats following intravenous injection for 1-24 hours at different time intervals

## Figures Legend

**Figure 1:**Three-dimensional (3D) response surface (A, C and E) and contour plots (B, D and F), showing the effects of lipid concentration, drug percentage and surfactant ratio on PDI of the astaxanthin nanoformulation.

**Figure 2:** (a) Particle size distribution of prepared astaxanthin solid lipid nanoparticles (AST-SLN). (b) Scanning electron microscopy (SEM) of prepared astaxanthin solid lipid nanoparticles (AST-SLN). (c) Transmission electron microscopy (TEM) of prepared astaxanthin solid lipid nanoparticles (AST-SLN).

**Figure 3:** In-vitro release of astaxanthin from the SLN's as a function of time at different time intervals (0-48 hrs) by using dialysis method in phosphate buffer at pH 7.4.

**Figure 4:** Scientigraphy image of Wistar rat 1 h after intravenous (a) and intranasal (b) administration of 99mTc-AST-SLN for localization of 99mTc-AST-SLN in different organ and tissues of experimental subject.

**Figure 5:** Dose standardization of AST-SLN and percentage cell survival by MTT assay.

**Figure 6:** Comparative analysis of AST-SLN on $H_2O_2$ induced oxidative stress in PC12 cells.

**Figure 7:** Effect of astaxanthin formulation on hydrogen peroxide induced alterations in the levels of intracellular GSH concentrations.

**Figure 8:** Effect of astaxanthin formulation on hydrogen peroxide induced alterations in the levels of intracellular lipid per oxidation.

**Table 1:** Levels of formulation parameters (A) lipid concentration (B) Amount of drug % (C) surfactant ratio used in Box-Behnken's response surface design of astaxanthin solid lipid nanoparticles.

| Formulation Parameters | Levels | | |
|---|---|---|---|
| | -1 | 0 | +1 |
| Lipid Concentration ($g100ml^{-1}$) | 50 | 150 | 250 |
| Amount of Drug (%) | 3 | 8 | 13 |
| Poloxamer: Lecithin | 100:50 | 200:50 | 300:50 |

**Table 2:** Box-Behnken's design with actual and predicted values of particle size (PS) and poly dispersity index (PDI) for astaxanthin solid lipid nanoparticles

| S. No | Lipid Concentration (mg) | % Amount of drug | Ratio of Poloxamer: Lecithin | PS | | PDI | |
|---|---|---|---|---|---|---|---|
| | | | | Actual | Predicted | Actual | Predicted |
| 1 | 50 | 3 | 200:50 | 174 | 199.45 | 0.354 | 0.581 |
| 2 | 250 | 3 | 200:50 | 1658 | 1539.25 | 0.798 | 0.798 |
| 3 | 50 | 13 | 200: 50 | 182.9 | 301.65 | 0.853 | 0.852 |
| 4 | 250 | 13 | 200: 50 | 1958 | 1932.55 | 0.864 | 0.636 |
| 5 | 50 | 8 | 100: 50 | 377.7 | 268.4 | 0.569 | 0.473 |
| 6 | 250 | 8 | 100: 50 | 1684 | 1718.9 | 0.214 | 0.346 |
| 7 | 50 | 8 | 300: 50: | 172 | 137.1 | 0.569 | 0.436 |
| 8 | 250 | 8 | 300: 50 | 1548 | 1657.3 | 0.468 | 0.563 |
| 9 | 150 | 3 | 100: 50 | 259 | 342.85 | 0.542 | 0.409 |
| 10 | 150 | 13 | 100: 50 | 1093 | 1083.55 | 0.123 | 0.218 |
| 11 | 150 | 3 | 300: 50 | 729.9 | 739.35 | 0.349 | 0.253 |
| 12 | 150 | 13 | 300: 50 | 578 | 494.15 | 0.421 | 0.553 |
| 13 | 150 | 8 | 200: 50 | 789 | 682 | 0.224 | 0.224 |
| 14 | 150 | 8 | 200: 50 | 584 | 682 | 0.224 | 0.224 |
| 15 | 150 | 8 | 200: 50 | 729 | 682 | 0.224 | 0.224 |
| 16 | 150 | 8 | 200: 50 | 654 | 682 | 0.224 | 0.224 |
| 17 | 150 | 8 | 200: 50 | 654 | 682 | 0.224 | 0.224 |

**Table 3:** Analysis of variance of calculated model of astaxanthin solid lipid nanoparticles for particle size and poly dispersity index.

| | Size | PDI |
|---|---|---|
| **Regression** | | |
| Sum of square | 5192813 | 0.710103 |
| Df | 9 | 9 |
| Mean squares | 576979.2 | 0.0789 |
| F value | 42.56005 | 2.623971 |
| P | <0.0001 | 0.1085 |
| **Residual** | | |
| Sum of square | 94897.78 | 0.210483 |
| Df | 7 | 7 |
| Mean square | 13556.83 | 0.030069 |
| **Lack of fit test** | | |
| Sum of square | 70067.78 | 0.210483 |
| Df | 3 | 3 |
| Mean squares | 23355.93 | 0.070161 |
| F value | 3.762533 | - |
| P value | 0.1166 | - |
| Coefficient correlation ($r^2$) | 0.982053 | 0.771359 |
| Coefficient of variation (CV %) | 14.31787 | 40.69399 |
| Adequate precision value | 20.10568 | 4.770856 |

**Table 4:** Bio-distribution of 99mTc AST-SLN in Wister rats following intranasal injection for 1-24 hours at different time intervals.

| Organ | Percent injected dose/gram organ (± SEM) | | | |
|---|---|---|---|---|
| | 1hr | 2hr | 4hr | 24hr |
| Blood | 0.50±0.04 | 0.345±0.05 | 0.309±0.03 | 0.065± 0.002 |
| Heart | 0.27± 0.07 | 0.21± 0.01 | 0.16± 0.03 | 0.094± 0.007 |
| Lung | 0.48± 0.21 | 0.35± 0.12 | 0.31± 0.16 | 0.055± 0.05 |
| Liver | 1.07± 0.39 | 0.83± 0.26 | 0.573± 0.17 | 0.096± 0.06 |
| Spleen | 0.41± 0.12 | 0.335± 0.09 | 0.21± 0.08 | 0.043± 0.001 |
| Kidney | 0.88± 0.09 | 0.67± 0.06 | 0.34± 0.04 | 0.089± 0.001 |
| Stomach | 6.6± 0.68 | 4.48± 0.6 | 1.98± 0.22 | 0.049± 0.003 |
| Intestine | 20.06±1.08 | 14.84±0.97 | 9.02±0.24 | 1.49±0.16 |
| Brain | 1.70±0.13 | 1.34±0.11 | 1.1±0.17 | 0.15±0.005 |

Data from four rats group expressed as % injected dose/gram organ ± SEM

**Table 5:** Bio-distribution of 99mTc AST-SLN in Wister rats following intravenous injection for 1-24 hours at different time intervals..

| Organ | Percent injected dose/gram organ (± SEM) | | | |
|---|---|---|---|---|
| | 1hr | 2hr | 4hr | 24hr |
| Blood | 0.87 ± 0.12 | 0.67 ± 0.15 | 0.61 ± 0.09 | 0.075 ± 0.004 |
| Heart | 0.38 ± 0.03 | 0.31 ± 0.03 | 0.27 ± 0.01 | 0.019 ± 0.001 |
| Lung | 0.36 ± 0.07 | 0.29 ± 0.06 | 0.21 ± 0.02 | 0.030 ± 0.001 |
| Liver | 1.08 ± 0.05 | 0.91 ± 0.01 | 0.59 ± 0.08 | 0.087 ± 0.05 |
| Spleen | 0.59 ± 0.06 | 0.52 ± 0.41 | 0.31± 0.02 | 0.036 ± 0.003 |
| Kidney | 0.78 ± 0.05 | 0.69 ± 0.10 | 0.63 ± 0.03 | 0.006 ± 0.002 |
| Stomach | 8.172± 1.01 | 6.5± 0.63 | 3.1± 0.56 | 0.080± 0.001 |
| Intestine | 7.76 ± 0.60 | 5.73± 0.70 | 3.98±0.02 | 0.467±0.27 |
| Brain | 0.844 ± 0.12 | 0.72± 0.18 | 0.61±0.09 | 0.086±0.08 |

Data from four group expressed as % injected dose/gram organ ± SEM

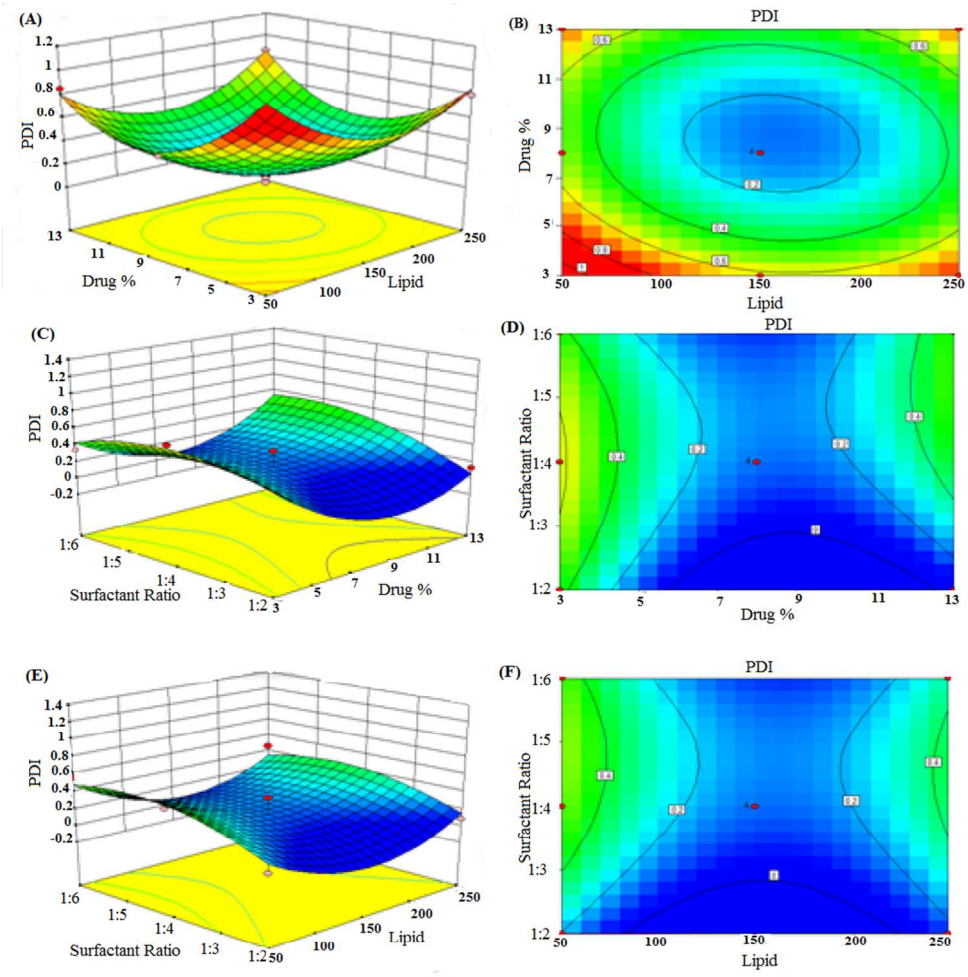


**Figure 1:** Three-dimensional (3D) response surface (A, C and E) and contour plots (B, D and F), showing the effects of lipid concentration, drug percentage and surfactant ratio on PDI of the astaxanthin nanoformulation.

288x331mm (96 x 96 DPI)

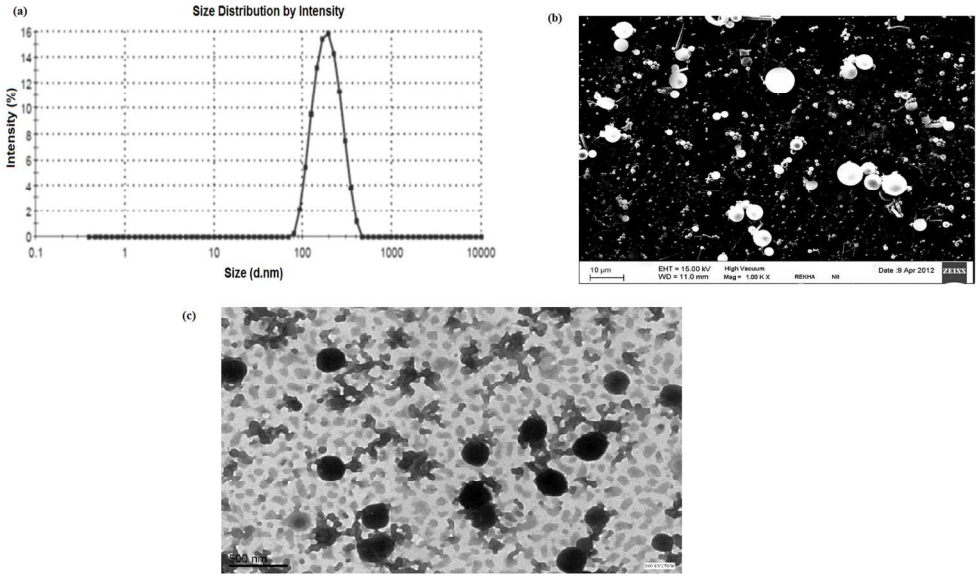


**Figure 2:** (a) Particle size distribution of prepared astaxanthin solid lipid nanoparticles (AST-SLN). (b) Scanning electron microscopy (SEM) of prepared astaxanthin solid lipid nanoparticles (AST-SLN). (c) Transmission electron microscopy (TEM) of prepared astaxanthin solid lipid nanoparticles (AST-SLN).

920x713mm (96 x 96 DPI)

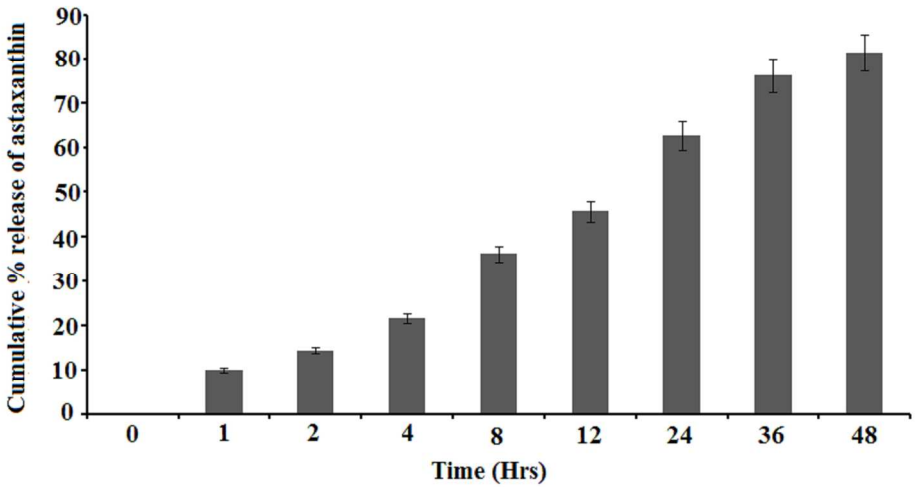


**Figure 3:** In-vitro release of astaxanthin from the SLN's as a function of time at different time intervals (0-48 hrs) by using dialysis method in phosphate buffer at pH 7.4.

439x280mm (96 x 96 DPI)

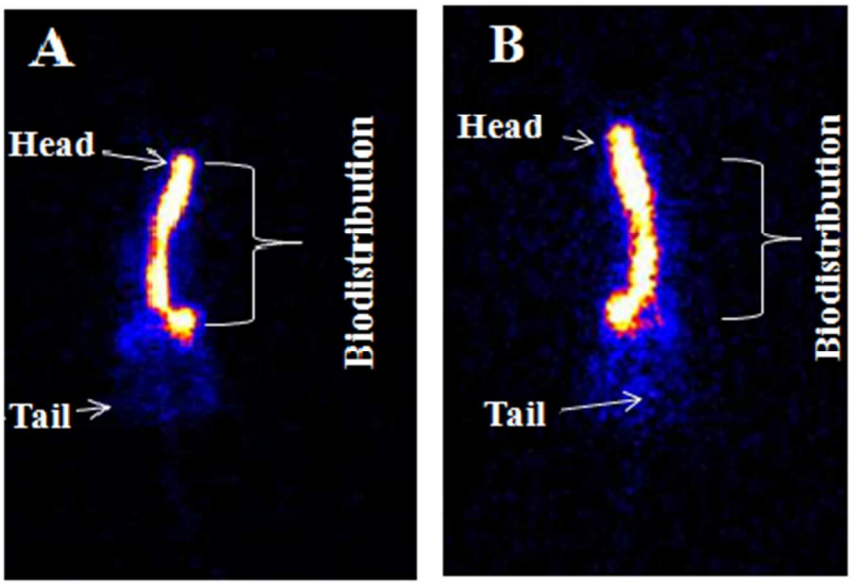


**Figure 4:** Scientigraphy image of Wistar rat 1 h after intravenous (a) and intranasal (b) administration of 99mTc-AST-SLN for localization of 99mTc-AST-SLN in different organ and tissues of experimental subject.

117x109mm (96 x 96 DPI)

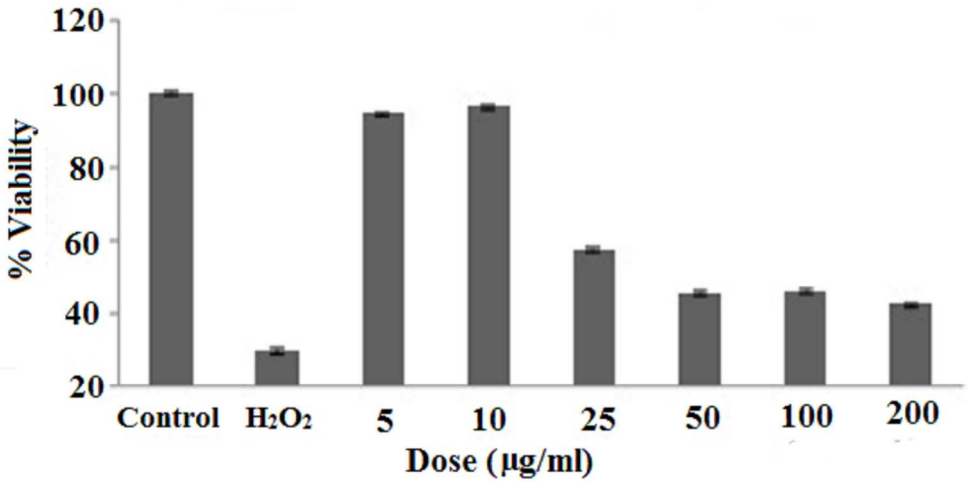


**Figure 5:** Dose standardization of AST-SLN and percentage cell survival by MTT assay

324x190mm (96 x 96 DPI)

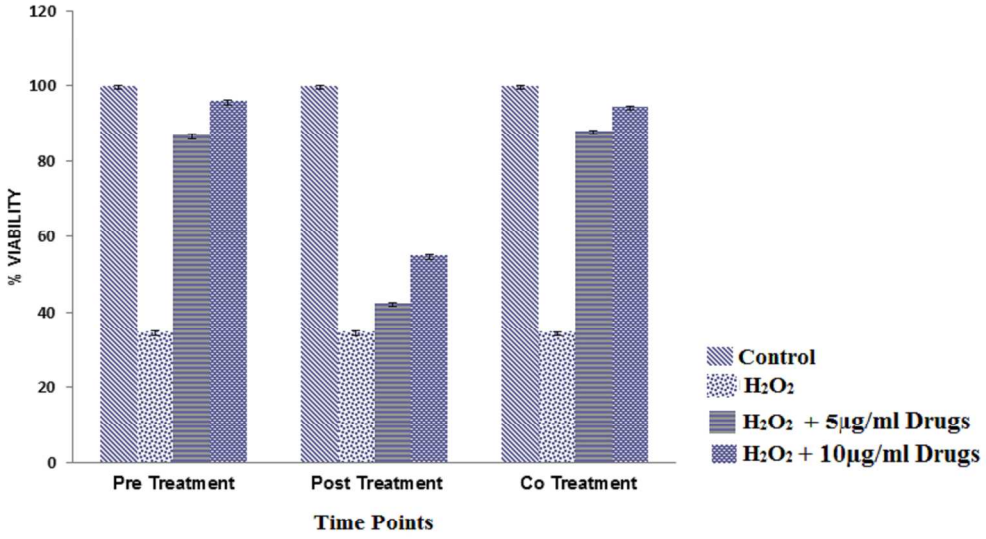


**Figure 6:** Comparative analysis of AST-SLN on $H_2O_2$ induced oxidative stress in PC12 cells

430x291mm (96 x 96 DPI)

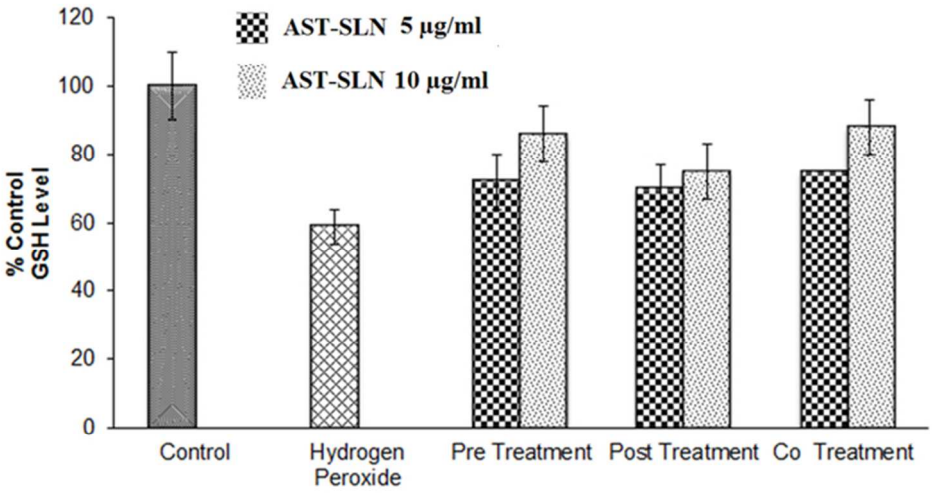


**Figure 7:** Effect of astaxanthin formulation on hydrogen peroxide induced alterations in the levels of intracellular GSH concentrations.

63x40mm (300 x 300 DPI)

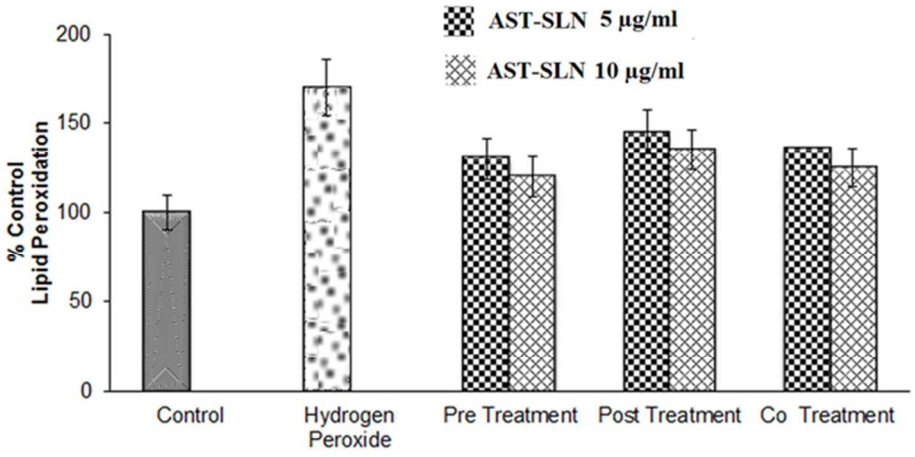


**Figure 8:** Effect of astaxanthin formulation on hydrogen peroxide induced alterations in the levels of intracellular lipid per oxidation.

63x38mm (300 x 300 DPI)

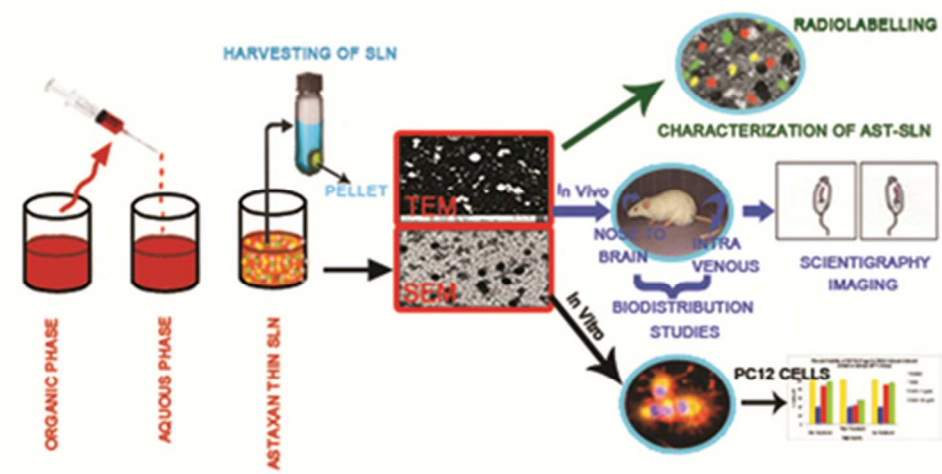


The prepared astaxanthin nano-formulation was found to be appropriate in all measures and was found to be free of any adverse effects. The formulation showed strong antioxidant activity in Pheochromocytoma cell lines against H2O2 induced oxidative stress. Biodistribution and brain delivery of the drug was found to be very promising as compared to the conventional dosage form.
39x19mm (300 x 300 DPI)